



The descending motor tracts are different in dancers and musicians

Chiara Giacosa^{1,2} · Falisha J. Karpati^{1,3} · Nicholas E. V. Foster^{1,4} · Krista L. Hyde^{1,3,4} · Virginia B. Penhune^{1,2}

Received: 12 February 2019 / Accepted: 1 October 2019 / Published online: 16 October 2019
© Springer-Verlag GmbH Germany, part of Springer Nature 2019

Abstract

Long-term motor training, such as dance or gymnastics, has been associated with increased diffusivity and reduced fiber coherence in regions including the corticospinal tract. Comparisons between different types of motor experts suggest that experience might result in specific structural changes related to the trained effectors (e.g., hands or feet). However, previous studies have not segregated the descending motor pathways from different body-part representations in motor cortex (M1). Further, most previous diffusion tensor imaging studies used whole-brain analyses based on a single tensor, which provide poor information about regions where multiple white matter (WM) tracts cross. Here, we used multi-tensor probabilistic tractography to investigate the specific components of the descending motor pathways in well-matched groups of dancers, musicians and controls. To this aim, we developed a procedure to identify the WM regions below the motor representations of the head, hand, trunk and leg that served as seeds for tractography. Dancers showed increased radial diffusivity (RD) in comparison with musicians, in descending motor pathways from all the regions, particularly in the right hemisphere, whereas musicians had increased fractional anisotropy (FA) in the hand and the trunk/arm motor tracts. Further, dancers showed larger volumes compared to both other groups. Finally, we found negative correlations between RD and FA with the age of start of dance or music training, respectively, and between RD and performance on a melody task, and positive correlations between RD and volume with performance on a whole-body dance task. These findings suggest that different types of training might have different effects on brain structure, likely because dancers must coordinate movements of the entire body, whereas musicians focus on fewer effectors.

Keywords Neuroplasticity · Motor training · Probabilistic tractography · Descending motor pathways or corticospinal tract or pyramidal tracts · White matter · Dance and music

Introduction

Studies with dancers and athletes, using diffusion-weighted imaging (DWI), point toward an association between expertise and changes in white matter (WM) architecture. In

particular, in a recent paper we showed that highly trained dancers have increased diffusivity and reduced fiber coherence in the corticospinal tract, superior longitudinal fasciculus and the corpus callosum in comparison with musicians (Giacosa et al. 2016). Similar findings have been reported in other studies of dancers and athletes (Jäncke et al. 2009; Hänggi et al. 2010; Huang et al. 2013; Meier et al. 2016; Burzynska et al. 2017). In comparison, studies in trained musicians have generally reported focal increases in measures of fiber coherence (Han et al. 2009; Halwani et al. 2011; Rüber et al. 2013; Acer et al. 2018). Reduced measures of WM coherence in dancers and athletes have been interpreted as an increase in crossing or fanning of fibers and attributed to enhanced connectivity between sensorimotor regions representing different body parts. In contrast, the focal increases observed in musicians may represent increased coherence resulting from intensive training of specific effectors (e.g., hands). In the current study, we test these hypotheses in a

✉ Chiara Giacosa
chiagiarasa@gmail.com

¹ International Laboratory for Brain, Music and Sound Research (BRAMS), Pavillon 1420 Mont Royal, CP 6128, Succ. Centre Ville, Montreal, QC H3C 3J7, Canada

² Department of Psychology, Concordia University, 7141 Sherbrooke Street West, Montreal, Quebec H4B 1R6, Canada

³ Faculty of Medicine, McGill University, 3655 Sir William Osler, Montreal, Quebec H3G 1Y6, Canada

⁴ Department of Psychology, University of Montreal, Pavillon Marie-Victorin, 90 avenue Vincent d'Indy, Montreal, Quebec H2V 2S9, Canada

sample of highly trained musicians and dancers using probabilistic tractography to examine the connectivity of different body-part representations in the motor cortex (M1). To do this, we developed a novel procedure to identify the seed regions for the hand, trunk/arm, leg and head in M1. Those regions were then used as seeds to track sub-divisions of the descending primary motor pathways and compare diffusion parameters and volumes between dancers and musicians.

Most of the previous research (Hänggi et al. 2010; Giacosa et al. 2016; Burzynska et al. 2017) is based on whole-brain analyses, which provide global information about the location of WM changes, but cannot tell us about the specific connections from individual regions. Moreover, the most common diffusion tensor imaging (DTI) model assumes that all fibers in each voxel follow the same direction (Basser et al. 1994), which is less accurate in regions with many crossing fibers. In contrast, probabilistic tractography based on a multi-tensor model allows the reconstruction of individual fiber tracts (Behrens et al. 2007).

There is a large body of evidence showing neural plasticity of gray (GM) and white matter in sensorimotor regions of novices who undergo short-term training (Draganski et al. 2004; Scholz et al. 2009; Taubert et al. 2010, 2016; Bezzola et al. 2011; Sampaio-Baptista et al. 2013), as well as of trained dancers, musicians and athletes (Schlaug et al. 1995; Gaser and Schlaug 2003; Jäncke et al. 2009; Hänggi et al. 2010; Wang et al. 2013; Steele et al. 2013; Schlaffke et al. 2014; Bailey et al. 2014; Huang et al. 2013; Burzynska et al. 2017; Karpati et al. 2017). Training studies in both animals and humans show local reorganization of the specific representations of the trained effectors (e.g., Karni et al., 1995; Kleim et al., 2002; Kleim et al., 1998; Morgen et al., 2004; Nudo et al., 1996; Taubert et al., 2016). Similarly, most studies with trained musicians, dancers or other athletes found enlargements in the motor representation of the trained effectors (Elbert et al. 1995; Pantev et al. 2001; Tyč et al. 2005; Vaalto et al. 2013; Choi et al. 2015; Meier et al. 2016), and/or changes in WM motor pathways (Bengtsson et al. 2005; Han et al. 2009; Imfeld et al. 2009; Wang et al. 2013; Rüber et al. 2015; Giacosa et al. 2016; Acer et al. 2018), linked to the effector used (Meier et al. 2016). In particular, professional dancers and gymnasts, whose training involves comparably complex whole-body movements, had lower fractional anisotropy (FA) in sensorimotor and interhemispheric motor pathways which was attributed to greater axon diameter, increased crossing or fanning of fibers, or more wide-spread connectivity (Hänggi et al. 2010; Huang et al. 2013; Giacosa et al. 2016; Burzynska et al. 2017). Conversely, long-term music training has frequently been associated with increased FA in the corticospinal tract (CST) (Bengtsson et al., 2005; Han et al., 2009; Rüber et al., 2015, but see Imfeld et al., 2009; Schmithorst and Wilke, 2002), and in the arcuate fasciculus (Halwani et al. 2011). In a previous study (Giacosa et al. 2016), using tract-based spatial statistics

(TBSS), we showed that dancers had higher radial diffusivity (RD) values, while musicians had higher FA, in a variety of regions, including the CST. Interestingly, controls' RD and FA values fell between the two expert groups, suggesting opposite associations between dance or music training and WM microstructure. Consistent with these findings, Meier et al. (2016) observed lower FA and higher RD values in ballet dancers in comparison with handball players, especially in the tract seeded in the motor cortex region that included the representation of the leg/foot. Lower FA and higher RD might indicate greater fiber crossing or increased axon diameter within this tract. Together with our own results, this points to enhanced connectivity among a broader selection of brain regions for dancers, in contrast to enhanced connectivity in more focal sets of connections for musicians.

To test this hypothesis, in the current study we used a multi-tensor probabilistic tractography approach to compare the primary motor pathways in professional dancers and musicians with a similar amount of training. The TBSS approach that we previously used is based on the whole-brain diffusion single-tensor model (Basser et al. 1994), which only represents one fiber direction. Conversely, the multi-tensor probabilistic tractography (Behrens et al. 2003) can model more than one possible fiber direction, allowing for a better assessment of tracts in regions with multiple crossing fibers, such as certain portions of the CST. We therefore used two-fiber probabilistic tractography to identify the motor pathways descending from the head, hand, trunk/arm and leg/foot motor regions. To do this, we first identified the motor hand areas in each participant based on gross anatomical landmarks (Yousry et al. 1997; Caulo et al. 2007). The ROIs for the trunk/arm, leg and head areas were created relative to this location. Seed masks based on these ROIs were placed in the subjacent WM because tracking from WM is more reliable than from GM, where the orientation of fibers is neither coherent nor clearly detectable. We then tracked the fiber bundles connecting these regions to the cerebral peduncles and extracted diffusivity and volumetric measures across the entire tracts, as well as in the WM seed masks and the posterior limb of internal capsules (PLIC). This allowed us to test the hypothesis that dancers might have increased connectivity across all the body-part representations, whereas musicians might have more focused connectivity with the hand region.

Materials and methods

Participants

Three groups of participants (age 18–40) were recruited for this study: trained dancers ($N = 20$), trained musicians ($N = 19$) and a control group of non-musician/non-dancers

($N = 20$). This is the same sample used in our previous studies examining WM and GM structure in dancers and musicians using whole-brain approaches (Giacosa et al. 2016; Karpati et al. 2016, 2017, 2018). Groups did not differ in age, sex distribution, body mass index (BMI) or years of education (Table 1). Participants had no past or current developmental, neurological or psychiatric disorder, nor reported any alcohol or substance abuse. Dancers and musicians were either currently practicing as professionals, or students involved in professional training. Their training was assessed via a detailed questionnaire developed in our laboratory, the Montreal Dance and Music History Questionnaire (MDMHQ) (Karpati et al. 2016), based on (Bailey and Penhune 2010; Coffey et al. 2011). Dancers and musicians had, on average, approximately 15 years of training in their respective disciplines, with a variety of training backgrounds. Controls had, on average, less than one year in dance, music, figure skating or aerobics experience (see Table 1). All participants were physically active (biking, running or practicing other physical exercises), and none had absolute pitch. Since the dance imitation task described below (see General procedures section) was based on a video game, participants were excluded if they had more than 2 years of experience with dance video-games.

One participant in each group was excluded: one dancer and one musician presented scan-related artefacts in the x-direction of raw data (see Giacosa et al., 2016), and one control had to be excluded because tractography failed to find any tract. The experimental protocol was approved by the Research Ethics Board at the Montreal Neurological Institute and Hospital, and a written informed consent was obtained from all participants. All participants were compensated for their participation.

General procedures

Participants took part in two testing sessions distributed over two non-consecutive days: one for behavioral testing and the other for MRI acquisition, including DWI images. The behavioral battery included dance- and music-related tasks as well as tests of global cognitive and memory function (described in more detail in Karpati et al. 2016). The dance imitation task was developed in our laboratory based on the video game Dance Central one for the console Xbox Kinect 360 (Harmonix, <http://www.harmonixmusic.com>) to assess the ability to observe and imitate in real time whole-body dance movements synchronized with music (Karpati et al. 2016). The melody discrimination task (Foster and Zatorre 2010) assesses auditory processing and pitch discrimination. Furthermore, a language task and three standardized cognitive tests were given to all participants to examine any possible group differences in global cognitive or memory function (Karpati et al. 2016).

Brain imaging and analysis

Diffusion and T1 image acquisition

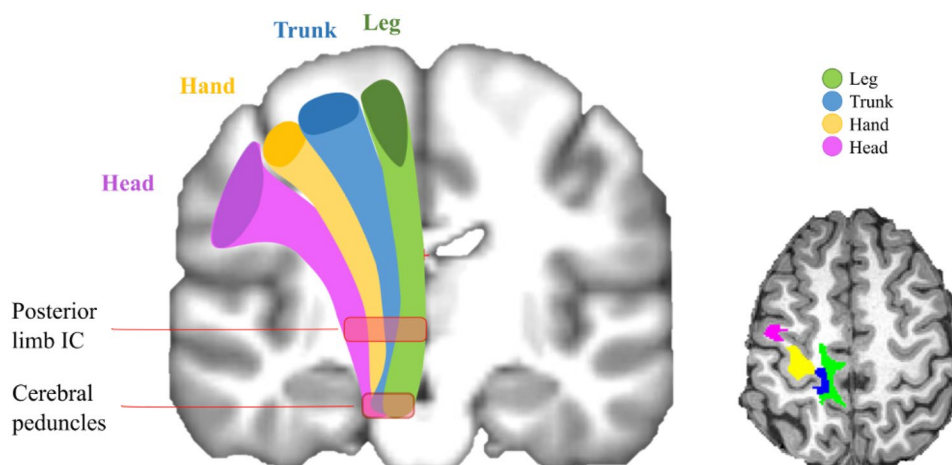
Diffusion-weighted (DWI) and T1 images were acquired for all participants at the Montreal Neurological Institute (MNI) on a 3T Siemens Trio MR scanner with a 32-channel head coil. The following parameters were applied: 99 diffusion-weighted gradient directions with a b -value of 1000 s/mm^2 , 10 b_0 non-weighted images, TE of 88 ms, TR of 9340 ms, EPI factor 128, isotropic voxels of $2 \times 2 \times 2 \text{ mm}^3$, 72 slices, FOV of 256 mm. T1-weighted brain images were acquired with the following parameters: echo time = 2.98 ms, repetition time = 2300 ms, voxel size 1 mm^3 . Ear plugs and headphones, as well as foam pads, were used to reduce noise perception and head motion, respectively.

Tractography procedure

We developed a procedure, combining FSL and Freesurfer tools, to separately track the motor pathways connecting the head, hand, trunk or leg regions. These tracts comprise the fibers that descend from the primary motor and premotor cortices to the brainstem (Fig. 1). In the current study, only the fibers originating in the WM subjacent M1 were tracked; in addition, the leg tracts included the fibers originating in the WM below both pre- and post-central cortices (M1 and S1, respectively) because the available parcellation of the paracentral cortices, provided by the Desikan-Killiany Atlas (Desikan et al. 2006), does not allow us to distinguish between them. To analyze diffusion and volumetric measures in the four bilateral distinct components of the primary motor pathways, we defined four seed masks per hemisphere, located in the WM immediately subjacent the M1 head, hand, trunk/arm, leg/foot representations, and the cerebral peduncles (see below and for a detailed description on how these masks were identified in “Supplementary Material”).

To do this, we first created a mask for the hand area based on anatomical landmarks (Yousry et al. 1997; Caulo et al. 2007) and then identified the trunk/arm, head and leg ROIs relative to that. These anatomically based ROIs likely contain multiple body-part representations: the hand ROI would also contain the fingers and wrist, the trunk/arm ROI would contain the representations of the trunk, shoulders and arm, the head ROI would contain the throat, face and neck representations, and the leg ROI would contain the leg, knee and foot representations. These WM ROIs were used as seed masks to track the portions of the primary motor pathways that connect each region to the ipsilateral cerebral peduncles (see Fig. 1). A three-voxel-thick slice, centered at $x = 0$ of the MNI space, was used as exclusion mask to avoid the confounding fibers of the corpus callosum.

Fig. 1 Reconstruction of the primary motor tracts for one hemisphere (left). The four seed masks are indicated in darker color in the WM below the motor cortex. The approximate location of the cerebral peduncles and of the posterior limb of the internal capsule (IC) is also shown with red boxes. Axial view of the WM seed masks in one subject's structural T1 image (right)



It is worth noting that separately tracking the descending tract components from each seed mask is more precise than tracking from the entire motor cortex and then dividing the whole tract into portions. Indeed, it would be impossible to identify the borders of the tract components along their length because they overlap. Moreover, tract shapes or sizes might differ between groups and along each tract component.

Diffusion preprocessing

The first steps of the DWI image preprocessing were previously explained (Giacosa et al. 2016). Briefly, individual raw data were corrected for eddy current distortions and head motion using the FMRIB's Diffusion Toolbox (FDT); then, non-brain voxels were excluded with the Brain Extraction Toolbox (BET) (Smith 2002), and the diffusion tensor model was applied (FDT) to estimate the diffusivity measures in each voxel. From the three eigenvalues, fractional anisotropy (FA) and radial (RD) diffusivities were calculated as the eccentricity of anisotropy and the average between the two lowest eigenvalues (RD), respectively. One subject per group was excluded from the analyses due to artefacts in the DTI data or outlier values.

Individual raw data were carefully checked. Due to scanning artefacts in the x-direction, some gradient directed frames (3D images) had to be excluded from the 4D individual images of 3/19 dancers, 5/18 musicians and 6/18 controls. This is a standard procedure in which the 4D image is split into multiple volumes, bad frames are removed, and the volumes are then recombined by merging the good frames. After correction, all subjects had between 79 and 99 gradient directed frames of good quality, except for one dancer who had 60 good frames. In all cases, the number of frames was good enough to allow full and reliable analyses for the entire sample. An average of all subjects' FA images was created in the $1 \times 1 \times 1 \text{ mm}^3$ MNI152 space, after linear (FLIRT)

(Jenkinson and Smith 2001; Jenkinson et al. 2002) and non-linear (FNIRT) transformations (Andersson et al. 2007) were applied to the individual FA images.

Probabilistic tractography

After modeling crossing fibers within each voxel of the brain with BedpostX (Behrens et al. 2007), a probabilistic two-fiber tractography approach was run with FSL ProbtrackX Tool (Behrens et al. 2003, 2007) to create connectivity distribution maps of the primary motor pathways in each subject. A connectivity distribution map indicates, at each voxel, how many streamline samples, originating from the seed mask, pass through that particular voxel and reach the target mask, avoiding the exclusion masks. Two fiber tracking procedures were executed for each tract: one to estimate the connectivity map (i.e., probability tractogram) originating in the seed mask and directed to the target and the other reconstructed in the opposite direction, from the target to the seed. The probability tractograms were normalized by dividing the number of streamline samples at each voxel by the total number of samples that reached the target (way-total) and then combined to obtain a defined tract, i.e., the probability of the union of the tractograms (P_{un}) (Andoh et al. 2015; Oechslein et al. 2017). Thus, a union tract (P_{un}) indicates the probability of tracking in both directions and was calculated according to the probability rules:

$$\begin{aligned} P_{\text{un}} &= P_{A \rightarrow B} \cup P_{B \rightarrow A} \\ &= P_{A \rightarrow B} + P_{B \rightarrow A} - (P_{A \rightarrow B} \cap P_{B \rightarrow A}), \end{aligned}$$

where

$$P_{A \rightarrow B} \cap P_{B \rightarrow A} = P_{A \rightarrow B} \times P_{B \rightarrow A}.$$

Individual P_{un} maps were then thresholded at 5% of the robust range of nonzero voxels ($\text{thrp} = 0.05$, multiplied by 100) and projected onto the standard FMRIB58_FA

Fig. 2 General steps followed to create the seed masks in one hemisphere. **a** User-drawn hand region (red) in one subject, axial view. **b** Average of user-drawn hand regions with center of gravity (COG) indicated as a black dot. **c** Spheres created from the COG of each body part, coronal view: hand sphere (yellow), trunk sphere (blue), leg sphere (green), head sphere (pink). The black dot is only an approximation of a COG with the red arrow showing the correspondence between the axial and coronal views. **d** The spheres (transparent colors) are overlapped with (opaque) masking of the WM regions subjacent the precentral cortex (PCC). **e** Final seed masks in one subject, diffusion FA space

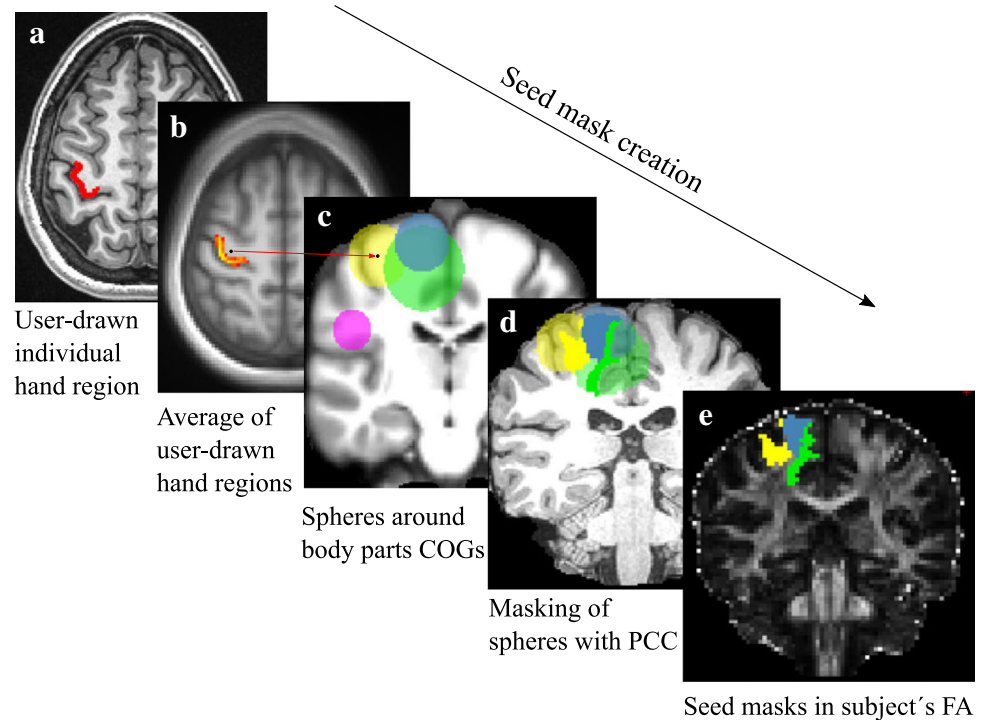


Table 1 Participant characteristics

Group	N	Age (yrs ± SD)	Sex	BMI (±SD)	Years of dance training (±SD)	Years of music training (±SD)	Level of education (±SD)
Dancers	19	25.1 ± 3.9	13F, 6M	21.6 ± 2.3	15.5 ± 5.2	1.7 ± 1.9	2.37 ± 0.6
Musicians	18	22.9 ± 3.4	12F, 6M	22.5 ± 3.2	1.04 ± 1.8	15 ± 3.6	2.39 ± 0.98
Controls	19	25.4 ± 5.1	12F, 7M	22.1 ± 3.1	0.4 ± 0.9	0.4 ± 1.0	2.58 ± 1.12
Comparison between groups	56	D=M=C Ns		D=M=C Ns	D>M=C P<0.0001	M>D=C P<0.0001	D=M=C Ns

Education levels for each group are calculated on a scale 1–5, where 1 is the lowest (completed high school) and 5 is the highest (completed PhD)

F females, M males, SD standard deviation, BMI body mass index.

template. The volume (V_{un}) of the thresholded P_{un} map was calculated as the number of the voxels in the FMRIB58_FA space (which corresponds to the MNI_1mm space).

In order to extract quantitative data from the tracts, the individual thresholded P_{un} were multiplied by each DTI measure (FA and RD) in the individual FA space and then projected on the common FMRIB58_FA template to allow for group comparisons. The DTI measures were then averaged across the entire tract, or across the extraction masks. To further investigate the volumetric properties of the tracts, two parts of each tract were identified: the core tract (T_{core}) and the dispersion tract (T_{disp}) (Oechslin2017). T_{core} is the part of the tract with the most consistent fiber bundle of the pathway and corresponds to the combined probability of both tracking directions; it was therefore calculated as the binarized intersection of the tractograms created in the opposite direction, which, in practical, means: $T_{core} = P_{A \rightarrow B} \times P_{B \rightarrow A}$.

In contrast, T_{disp} points to the more peripheral part of the fiber bundle, which is less consistent between the two tracking directions; to calculate it, the binarized T_{core} images were subtracted from the binarized unthresholded P_{un} : $T_{disp,bin} = P_{un,bin} - T_{core,bin}$. As before, T_{core} and T_{disp} were then transformed into the FMRIB58_FA space.

Definition of the seed and extraction masks

To create the seed masks for the four body-part regions in each hemisphere, we developed a procedure that included five main steps (see the diagram in “[Supplementary Material](#)”): (1) the localization of the hand regions, based on individual anatomical landmarks; (2) averaging of the individual hand maps to create a sphere based on the center of gravity for each hemisphere; (3) localization and creation of the spheres for the other body parts, relative to the hand

regions, on a template M1; (4) projection of the spheres on each individual space; (5) masking of the spheres with the individual parcellation of the WM subjacent M1 (Salat et al. 2009). This procedure is intended to be a good compromise between specificity and standardization across subjects.

As first step, the Freesurfer Recon-all Tool was applied to each subject's structural T1 image to calculate the individual parcellation of GM and WM, given in the individual Freesurfer conformed space. The obtained label of the precentral cortex (M1) served as visual guidance to manually draw each subject's hand region (Fig. 2a), according to the well-established landmarks of the hand knob (Yousry et al. 1997; Caulo et al. 2007). Individual T1 images were coregistered to the standard MNI152 (2mm) space via linear (FLIRT) and nonlinear (FNIRT) transformations and averaged across the entire sample to create a customized template. The Freesurfer Recon-all Tool was then applied to the template to calculate its GM-WM parcellation that served as a further guidance in the determination of the manually drawn initial hand masks. These initial masks of the hand regions were nonlinearly projected onto the template, averaged and thresholded at 30% (Fig. 2b, c), to calculate their center of gravity (COG) in each hemisphere. Two spheres of 15 voxels (voxel size = 1 mm³) were centered around these COGs ($x = 37$ mm, $y = -19$ mm, $z = 60$ mm in the right hemisphere; $x = -35$ mm, $y = -21$ mm, $z = 61$ mm in the left) to completely include the hand regions of the precentral cortex. These were then projected back to the individual structural T1 space from the template conformed space. Our sample-specific COGs were consistent with the centers of the spheres previously used for defining the hand and leg regions (Meier et al. 2016; Sehm et al. 2016). The hand spheres were appropriately shifted along M1 to create the head, trunk/arm and leg spheres. Since the regions containing the representations of the head and leg are more extended in the dorso-ventral direction, the radii of their spheres were adjusted accordingly (head radius: 24 mm; leg radius: 21 mm). The COG coordinates for the spheres were: $x = 14$ mm, $y = -25$ mm, $z = 66$ mm in the right hemisphere, and at $x = -13$ mm, $y = -25$ mm, $z = 66$ mm in the left, for the trunk spheres; $x = 49$ mm, $y = 3$ mm, $z = 25$ mm in the right hemisphere, $x = -46$ mm, $y = 3$ mm, $z = 25$ mm in the left, for the head spheres; $x = 13$ mm, $y = -25$ mm, $z = 54$ mm in the right hemisphere, $x = -13$ mm, $y = -25$ mm, $z = 54$ mm in the left, for the leg spheres. All spheres were then masked, in the individual T1 space, with the individual WM regions underlying M1, also transformed in the same space (Fig. 2d). To avoid overlapping, the trunk WM masks were subtracted from the hand WM masks. Finally, all WM masks were transformed into the individual diffusion space (FA) and used as seeds for tractography (Fig. 2e). The combined use of nonlinear transformations, employed to project

the spheres onto the individual space, and of the automated subcortical WM parcellation, used for masking the spheres, ensured that the selection of regions was subject-specific and consistent across subjects. More details on the procedure are reported in “Supplementary Material”.

Based on previous work (Giorgio et al. 2010), the cerebral peduncle seed masks were created by taking two symmetrical three-voxel-thick slices centered around $z = -22$ mm in the MNI152 1 mm space and limited to the area around the peduncles (x range: 0, -15; y range: -14, -46, z range: -21, -23). This binarized mask was then projected onto each subject's individual FA space and thresholded at the individual FA maps where $FA > 0.2$.

The masks described above were used to identify the primary motor tracts connecting specific body parts. Since the fiber bundle architecture might change along the tract, we aimed at analyzing these tracts at different levels: not only in its entirety (whole tract), but also in the WM seeds underlying the motor cortex and in the pLIC. The latter is a key region along the descending motor tracts, being the bottleneck where all fibers gather parallel and packed; thus, the pLIC is often examined as indicative of the entire CST. The pLIC ROIs were designed in the FMRIB_FA space as WM 3D boxes (x_{right} range: [20 mm, 28 mm], x_{left} range: [-19 mm, -27 mm], y range: [-13 mm, -26 mm], z range: [9 mm, 17 mm]) around the area labeled as ‘posterior limb of internal capsule’ by the JHU ICBM-DTI-81 White-Matter Labels atlas (Mori and Crain 2005).

Group comparisons

Once tractography was completed, all the quantitative measures were extracted from the whole probabilistic tracts and from the seed and pLIC ROIs described above. Although we analyzed several DTI metrics, (FA, RD, AD and MD), we will focus on RD and FA. Results from the analysis of AD and MD were largely consistent, and these values are correlated with those of RD and FA. For the DTI measures, the values of each voxel were averaged across the voxels of the ROIs used as extraction masks for each subject; for the volumetric measures (volume of the P_{un} tract = V_{un} , volume of T_{core} = V_{core} and volume of T_{disp} = V_{disp}), the number of voxels of the relevant extraction masks constituted the individual values to use for the inferential statistical analyses. The quantitative measures were compared between groups with ANCOVA analyses, in R ; age and sex were included as nuisance variables. Because no interaction effects were observed in the analyses where the main effects of group were significant, we calculated type II sums of squares for the ANCOVAs. To calculate pairwise group comparisons, adjusted for multiple comparisons, post hoc Tukey HSD tests were also performed.

Correlations with demographic and behavioral data

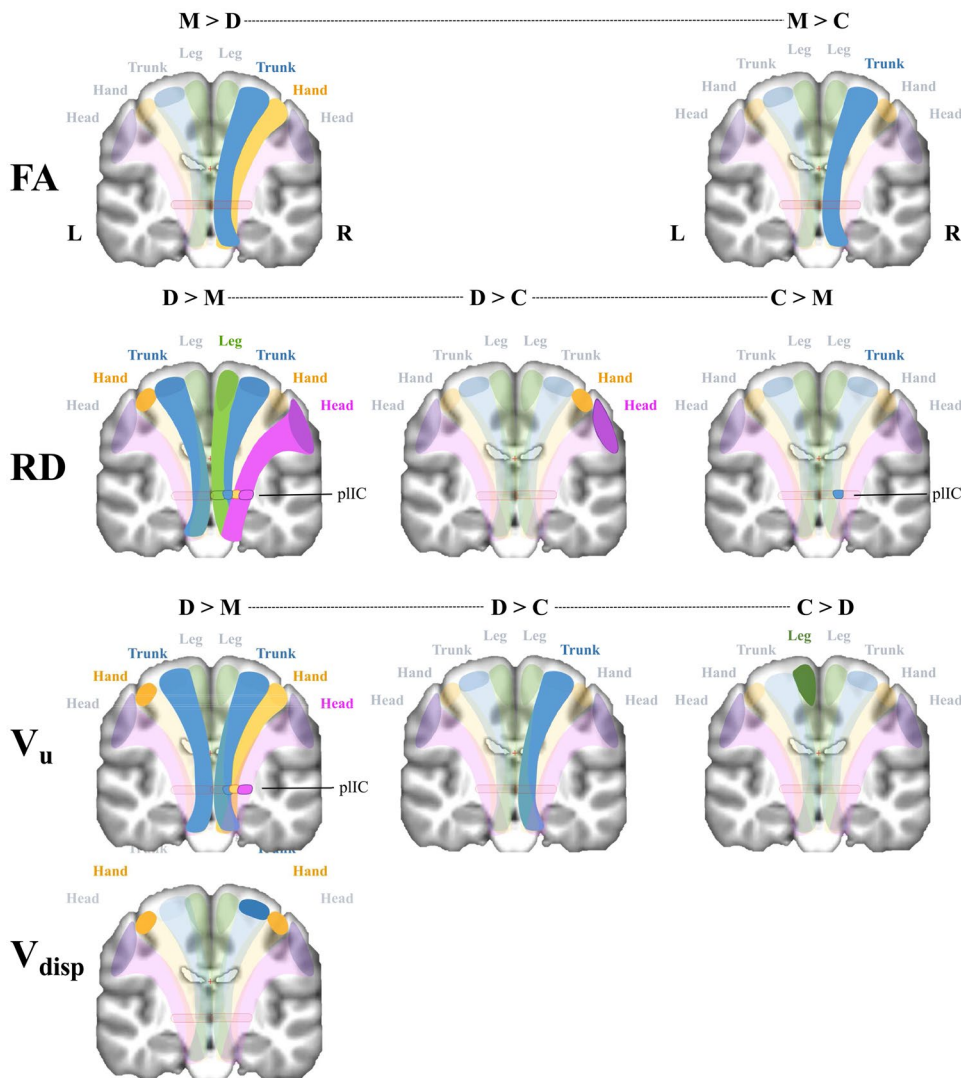
In order to estimate the associations between the brain data extracted from the hand, trunk and leg whole tracts and dance or music training, partial correlations were performed, within the groups of dancers or musicians separately, between the above-mentioned extracted values and: (1) dance or music training duration (calculated in number of years of training) or (2) age of start of dance or music training. Partial correlations were executed using the ppcor R package, following the Pearson correlation method and correcting for age and sex. The same partial correlation analyses were also performed between the brain data extracted from the whole tracts and performance on the dance and melody tasks.

Results

Group characteristics

As reported in previous papers, the groups did not differ in age, sex distribution, body mass index (BMI) or years of education, and dancers and musicians had a similar amount of training in their respective disciplines (see Table 1 and Giacosa et al., 2016; Karpati et al., 2016). These studies also showed that dancers outperformed musicians and controls on the dance task and that musicians performed better than dancers and controls on a melody discrimination task. Thus, the groups were well matched and demonstrated domain-specific expertise.

Fig. 3 Group comparison results. The opaque colors illustrate the portions of the tracts that differ between groups. The right hemisphere is shown on the right. R = right; L = left; D = dancers; M = musicians; C = controls; RD = radial diffusivity; FA = fractional anisotropy; V_u = volume of the union tract; V_{disp} = volume of the tract dispersion; pLIC = posterior limb of internal capsule



Tractography analyses

General information

Statistical analyses were conducted on the mean values extracted from the entire pyramidal tracts, the pLICs, as well as from the seed ROIs. For each analysis, DTI measures (fractional anisotropy (FA) and radial diffusivity (RD)) and volumetric measures (volume of the probability of the union of bidirectional streamlines (V_{un}), tract core volume (V_{core}), tract dispersion volume (V_{disp})) were analyzed. All reported results are significant at p -values < 0.05 , except where otherwise specified. Sex and age were included as covariates in all analyses.

Group differences

To assess effector-specific differences in the descending motor tracts, the DTI (FA and RD) and the volumetric measures (V_{un} , V_{core} , V_{disp}) were compared between groups for the whole tracts, the pLIC ROIs, often used as indicator for the entire CST, and the seed masks, where most group differences in crossing fibers might be expected. The tracts that significantly differed between groups are shown in Fig. 3; the statistical values are reported in Table 2. In general, RD values were higher in dancers and FA values were higher in

musicians and the majority of significant effects were found in the right hemisphere.

In the primary motor pathways seeded in the right hand region, across the entire tract, FA was higher in musicians in comparison with dancers, while V_{un} was bigger in dancers, with controls' values falling in between. In the pLIC, RD and V_{un} were both higher in dancers in comparison with musicians, and, in the hand ROI, RD and V_{disp} were higher. Control values fell between the two groups. For the primary motor pathways seeded in the right trunk/arm ROI, FA was higher in musicians compared to the other groups, whereas RD was higher in dancers versus musicians, and V_{un} was bigger in dancers compared to both other groups. For the pLIC, RD and V_{un} were lower in musicians in comparison with both controls and dancers. Finally, in the seed ROI, only V_{disp} was significantly larger in dancers in comparison with musicians. For the tract seeded in the leg region of the right hemisphere, RD was higher in dancers compared to musicians across the whole tract and in particular in the pLIC. No volumetric differences were found between groups. For the tracts seeded in the right head region, RD was higher in dancers. Consistent with this, in the pLIC of this tract, RD was higher and V_{un} was bigger in dancers compared to musicians. Similarly, in the head seed ROI, RD was higher in dancers compared to the other groups. No difference was found for V_{core} in any tract. Taken together, these results show that, for the tracts

Table 2 Statistical results of the group contrasts with age and sex included

Seed	Mask	RD				FA				V_{un}				V_{disp}				
		F _{2,50}	P	Part η^2	Tukey	F _{2,50}	P	Part η^2	Tukey	F _{2,50}	p	Part η^2	Tukey	F _{2,50}	P	Part η^2	Tukey	
Right	Trunk	Whole	3.817	0.029	0.132	D>M: 0.048	4.278	0.019	0.146	M>D: 0.002 M>C: 0.02	5.869	0.005	0.19	D>M: 0.006 D>C: 0.039				
		Seed													3.416	0.041	0.12	D>M: 0.018
		pLIC	9.858	0.0002	0.283	D>M: 0.001 C>M: 0.028					6.072	0.004	0.195	D>M: 0.005 C>M: 0.005				
	Hand	Whole					3.116	0.053	0.111	M>D: 0.014	3.314	0.045	0.117	D>M: 0.033				
		Seed	4.259	0.02	0.146	D>C: 0.024 D>M: 0.075									3.76	0.03	0.131	D>M: 0.008
		pLIC	4.189	0.021	0.144	D>M: 0.006					3.685	0.032	0.128	D>M: 0.006				
	Head	Whole	5.447	0.007	0.179	D>M: 0.006 D>C: 0.081												
		Seed	5.441	0.007	0.179	D>M: 0.024 D>C: 0.017												
		pLIC	4.384	0.018	0.149	D>M: 0.009												
	Leg	Whole	4.692	0.014	0.158	D>M: 0.045												
		pLIC	3.813	0.029	0.132	D>M: 0.032												
	Left	Trunk	Whole	3.796	0.029	0.132	D>M: 0.022											
Hand		Seed	4.246	0.02	0.145	D>M: 0.008	3.101	0.054	0.11	M>D: 0.052	3.65	0.033	0.127	D>M: 0.059	3.76	0.03	0.131	D>M: 0.006
Leg		Seed									3.311	0.045	0.117	C>D: 0.041				

F -values, p -values and partial eta squared (Part η^2) and the Tukey adjusted p -values are reported in the appropriate column. P -values slightly above the significant threshold of 0.05 are reported in italics. The columns F , p and Part η^2 indicate the values of the type II ANCOVAs with dancers (D), musicians (M) and controls (C) as levels for the factor GROUP, and age and sex included as covariates; the columns Tukey indicate the p -values of the post hoc Tukey tests in addition to the directionality of group difference (e.g., D > M meaning dancers greater than musicians). ROI = region of interest; Whole = whole tract (seeded in the corresponding Seed column); Seed = white matter seed ROI; pLIC = posterior limb of internal capsule. FA = fractional anisotropy; RD = radial diffusivity; V_{un} = volume of the union tract; V_{disp} = volume of the tract dispersion

Table 3 Significant brain-behavioral correlations for the tracts seeded in the right trunk and leg

Right Tract	Age of dance training start		Age of music training start		Dance performance (% correct)				Melody performance (% correct)	
	RD		FA		RD		V_{un}		RD	
	r	p	r	P	r	p	r	P	R	P
Trunk	-0.51	0.034	-0.52	0.037			0.33	0.015	-0.27	0.048
Leg					0.32	0.019				

RD radial diffusivity, FA fractional anisotropy, V_{un} volume of the tract union, r Pearson's correlation coefficient, p p -value, % correct percent correct

seeded in the right hand and trunk/arm regions, musicians have increased coherence and packing of fibers, across the entire bundles and particularly at the level of the pLIC of the trunk/arm tract. In contrast, dancers have increased dispersion of fiber orientation across the entire bundles. For the leg and head right motor pathways, dancers show greater diffusivity in every direction, likely suggesting an increase in the fiber orientation dispersion, especially below the cortex, and/or in the size of the axon diameter.

Left-hemisphere findings were more limited and largely consistent with those in the right hemisphere. In the left hand seed ROI, RD was higher and V_{disp} was bigger in dancers, whereas only a trend for smaller V_{un} was found in musicians in comparison with dancers. In the whole tract seeded in the left trunk, RD and V_{un} values were both higher in dancers in comparison with musicians. In the seed region of the same tract, no significant difference between groups was found neither in the V_{core} nor in the V_{disp} . No significant differences were found for either the head or leg regions. Together, these results are consistent with those of the right hemisphere, showing increased RD in the hand and trunk tracts of dancers, likely suggesting their reduced coherence and increased fiber orientation dispersion and/or augmented axon diameter.

Correlations with dance or music training

For the whole tracts of the hand, trunk and leg regions, where the groups differed, we examined the correlations of training variables with DTI and volume measures. Younger age of start for dancers was correlated with increased RD in the whole right trunk/arm tract, while younger age of start for musicians was associated with higher FA. No volumetric measures correlated with age of start of dance or music training. Of note, DTI measures were related to age of training start but not with years of training, although age of start and years of training were correlated for both dancers ($r = -0.59, p = 0.013$) and musicians ($r = -0.863, p < 0.0001$). In summary, consistent with the group differences, these results suggest that early start of

dance training is associated with increased RD, whereas early start of music training is associated with increased FA.

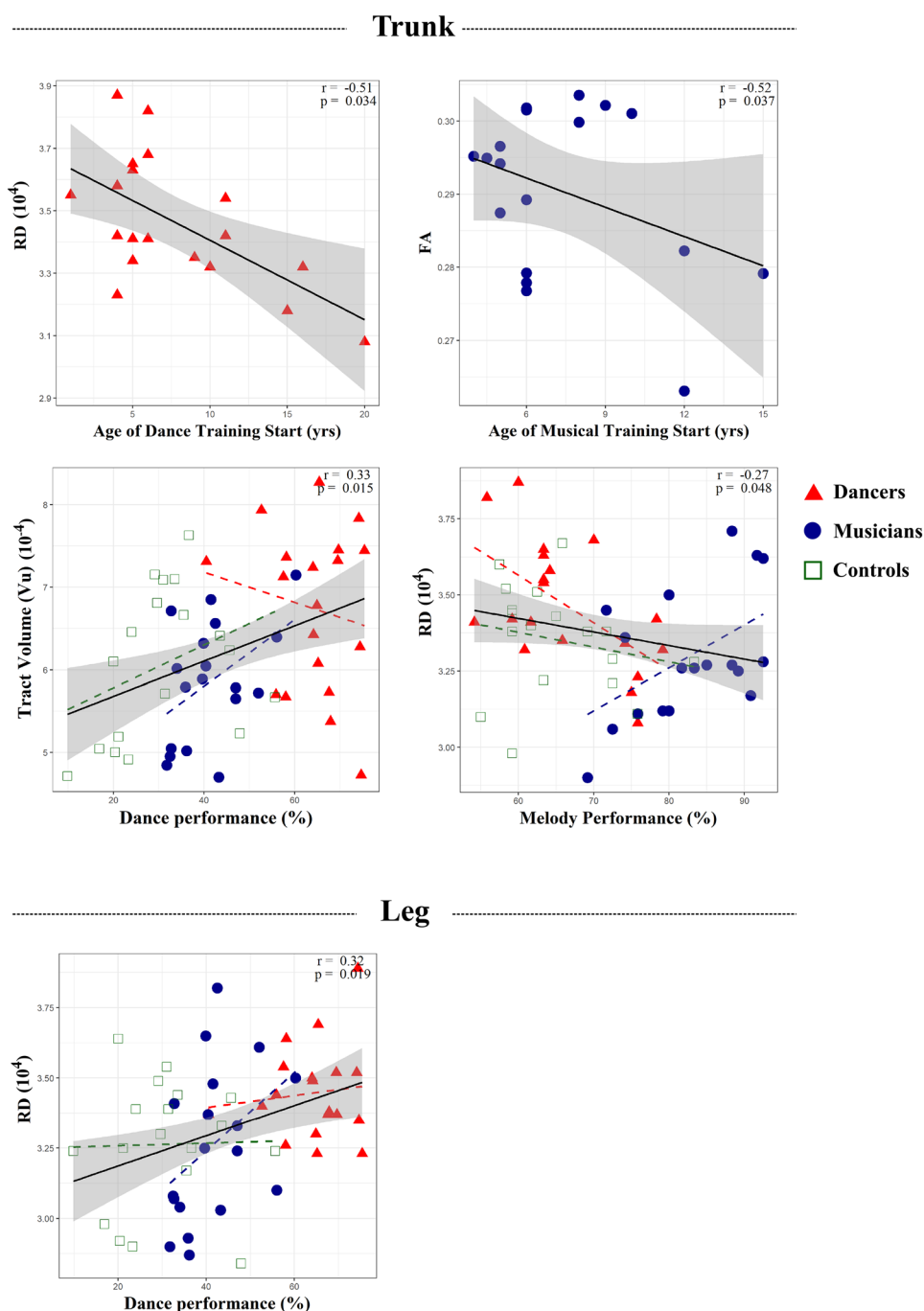
Correlations with dance or musical task performance

In order to confirm that the most relevant WM differences were related to dance and musical abilities, we calculated the partial correlations between quantitative measures, extracted from the entire hand, trunk and leg tracts in the right hemisphere, and performance on the dance and melody tasks (Karpati et al. 2016). Age and sex were included in the model as variables of no interest. As shown in Table 3 and Fig. 4, RD and the volume were positively correlated with performance on the dance task and negatively correlated with performance on the melody task, whereas FA did not correlate with any measure of task performance. In particular, in the entire right trunk tract, V_{un} was positively correlated with dance performance, while RD was negatively correlated with melody performance. Moreover, in the right leg tract, dance performance was positively correlated with RD across the whole tract.

Discussion

Using probabilistic two-fiber tractography, we showed that dancers had greater diffusivity (especially RD) in the primary motor pathways for all body regions in comparison with musicians, particularly in the right hemisphere. In contrast, musicians had greater anisotropy (FA) in the right hand and the trunk/arm tracts. Further, dancers had greater tract and dispersion volumes in these regions compared to both the other groups. The greater diffusivity and larger volumes observed in dancers might reflect increased fiber orientation dispersion, especially in proximity to the cortex, or increased axon diameter. In contrast, the higher FA values in musicians suggest increased coherence and packing of the fibers connecting the hand and arm motor representations. This confirms our hypothesis that dancers have broader connectivity in a larger number of regions, while musicians have more focused connections (Giacosa et al. 2016). Importantly, the observed differences in RD

Fig. 4 Correlations between WM and behavioral measures for the tracts seeded in the right trunk and leg. The dance-related measures are shown on the left column; the music-related measures are on the right. Shad-ows show the standard errors. *RD* radial diffusivity, *FA* fractional anisotropy, V_{un} volume of the union tract, r Pearson's correlation coefficient, p p -value, % percent correct



and *FA* were negatively correlated with the age of start of dance or music training, respectively. Finally, better dance performance was associated with increased diffusivity and volumetric measures, while better melody performance was associated with reduced *RD*.

Consistent with our previous study (Giacosa et al. 2016), we show that mean *RD* for dancers was higher in most of the primary motor pathways, particularly on the right. Increased *RD* in dancers might indicate enlarged axon diameter or enhanced fanning of the fiber bundles and is compatible with

a previous study comparing ballet dancers with handball players (Meier et al. 2016). Greater *RD* might result from use-dependent enlargement of axon diameter (Chéreau et al. 2017), and fibers with larger axon diameters are less packed, which would also contribute to increased *RD*. Higher *RD* is also compatible with greater fiber bundle branching or dispersion of fiber orientation. Greater branching in dancers might result from broader connectivity among representations of different body parts. Co-occurring movements are represented together in the primary motor cortex (Nudo et al.

1996); moreover, in the corticospinal tract, neurons originating in distinct, even non-contiguous, portions of M1 can converge, projecting to the same motor-neuron in the spinal cord (Hammond 2002). Therefore, the extraordinary variety of movement combinations learnt by dancers might lead to the encoding of a larger number of co-occurring movements and greater complexity of motor connections that would contribute to increasing the fanning of fibers. We observed higher RD in most tracts of dancers, in particular in the right leg. The leg tract is of peculiar relevance, given its fundamental involvement in dance training. This is consistent with Meier's and colleagues work (Meier et al. 2016), showing higher RD in the leg/foot component of ballet dancers' CST in comparison with handball players. Similar results were observed in the right head tract, where dancers showed increased RD, compared to both other groups. However, given the inherent non-specificity of diffusion measures (O'Donnell and Pasternak 2015), we cannot exclude other possible explanations for higher RD, such as decreased myelin thickness, changes in the axonal membrane permeability and internode distance (Sampaio-Baptista and Johansen-Berg 2017).

In comparison with dancers, musicians had higher FA values in the right hand and trunk/arm tracts. The result of concurrent higher FA in musicians and higher RD in dancers is consistent with previous findings in the CST when comparing dancers to musicians and other athletes (Giacosa et al. 2016; Meier et al. 2016). Importantly, musicians' FA values were also higher than controls in the trunk/arm tract, indicating that these changes were specific to musicians, and not just relative to the RD increases in dancers. Higher FA in the right CST (or pLIC) has been previously shown in musicians in comparison with controls (Acer et al., 2018; Han et al., 2009; Rüber et al., 2015, but see: Imfeld et al., 2009; Schmithorst and Wilke, 2002 for opposite findings), and it was associated with music training in childhood (Bengtsson et al. 2005). Here, the combination of higher FA and similar tract volume in musicians might be explained with increased coherence and packing of fibers (Wan and Schlaug 2010; Zatorre et al. 2012; Sampaio-Baptista and Johansen-Berg 2017). Indeed, musicians' specific training might increase the variety of movement representations within a single effector representation (e.g., hand), thus strengthening only those specific connections. The same findings can also be considered from the perspective that dancers, in both these tracts, showed lower FA and larger volume in comparison with musicians. Lower FA was previously observed in dancers and gymnasts (Hänggi et al. 2010; Huang et al. 2013; Giacosa et al. 2016; Meier et al. 2016; Burzynska et al. 2017) in comparison with non-dancers. The combination of bigger volume and lower FA in dancers supports the hypothesis of axon diameter augmentation with reduced packing of fibers, perhaps in combination with broader bundle fanning (see the concept of M1 fiber convergence in Hammond

2002). Taken together, our results demonstrate different types of plastic changes in the white matter of musicians and dancers: music training is associated with higher FA, which can be interpreted as stronger connectivity related to the specific effector trained, whereas dance training is associated with higher RD, which can be interpreted as enhanced connectivity across many effectors. To note that DTI metrics calculation derives from multiple preprocessing steps that reduce the test-retest reliability of DTI-based analyses (Madhyastha et al. 2014). Therefore, all DTI-based analyses should be interpreted with caution.

The finding that WM differences between dancers and musicians are predominantly right sided is consistent with the whole-brain findings of our previous study (Giacosa et al. 2016). While structural changes have also been observed in the left hemisphere both in our study and others, (Hänggi et al. 2010; Meier et al. 2016; Burzynska et al. 2017), we hypothesize that greater changes on the right are the result of greater training of the non-dominant left hand (Rüber et al. 2013), and the complexity and bilateral coordination of movements learned. For example, increased movement coordination and complexity likely require broader functional bilateral activity (Horenstein et al. 2009; Noble et al. 2014), and increasing complexity of finger tapping sequences was correlated with increased ipsilateral activation of motor regions (Harrington and Alan Fine 2000; Verstynen et al. 2005).

Importantly, correlations with age of training start give support to our findings. Younger age of start of dance training was negatively correlated with RD values in the entire right trunk tract, indicating that the earlier dance training started, the greater was the fiber orientation dispersion. In the same tract, age of start of music training was negatively correlated with FA, indicating that the earlier music training started, the more coherent were the fibers. Further, larger tract volumes were associated with better performance in the dance task. These correlations validate a stronger association between dance training and fiber orientation dispersion and axonal enlargement, in contrast to an association between music training and changes in fiber coherence and packing.

Considering that the same tract may present different fiber bundle configurations at different levels, one of the goals of the present study was to examine the primary motor pathways both where the tracts enter the cortex (seed ROIs) and at the level of the pLIC. Thinking of the fiber bundle as tree-shaped, in the pLIC, all fibers converge and run parallel to each other, like in the tree trunk; in contrast, in the seed regions, the multiplicity of neurons leaving the cortex constitutes the broad branching foliage of the fiber bundles. In the present study, in the right pLIC of the head and hand tracts, dancers had higher RD and V_{wm} in comparison with musicians. Dancers' larger motor axons, although more packed in the lower tract portions of the pLIC compared to

the seed regions, might be less organized than the highly packed fibers of musicians, resulting in increased RD and larger volume. In addition, their more extensive combination of co-executed movements might require several M1 fibers to connect to the same motor-neurons, possibly explaining the ‘thicker tree trunk’, or bigger pLIC volume. In contrast, musicians’ trunk/arm pLIC had lower RD values and smaller volume compared to both dancers and controls. This could reflect particularly myelinated, coherent and packed fibers, supporting the hypothesis of a more sharply defined tract morphology in the CST of musicians, as suggested by Oechslin (2017).

Another interesting finding is that dancers showed higher RD and V_{disp} in the hand and trunk seed ROIs bilaterally. It is worth reminding that each fiber tract was tracked bidirectionally, from the seed to the target and vice versa. Thus, the V_{disp} included only the voxels that contained the non-overlapping streamlines obtained from tracking in only one of the two directions, i.e., from seed to target or the opposite (dispersion tract, T_{disp}). The increased dispersion of fiber orientation is likely the consequence of microstructural properties, such as greater incoherence of fibers in dancers. This might be particularly true in the seed regions, not only because these are larger ROIs than the cerebral peduncles, but also because they lie right below the cortex, where is the maximal incoherence of fibers. Furthermore, the greater V_{disp} observed in dancers might reflect their increased fiber orientation dispersion, or the fact that the tracts might be more easily identified in one direction or the other (from the cortex to the cerebral peduncles or the opposite).

Training effects or preexisting differences?

Differences in brain structure between dancers and musicians have generally been attributed to long and intensive training. However, it is more likely that they result from an interaction between training-induced plasticity and preexisting differences in physical characteristics, brain structure or personality traits that predispose certain people to engage in one or the other discipline (see Penhune 2019). However, while comparisons between trained and non-trained groups might be confounded by differences in environmental factors such as motivation, familiarity, or personality traits like perseverance, given the similar intensity of training required by both disciplines, it is highly plausible that such factors are similar in dancers and musicians. Therefore, the brain differences observed between these groups are more likely attributable to the specific training. Future longitudinal or targeted cross-sectional studies may more directly address the issue of distinguishing between the training-induced changes versus predispositions.

Advantages of our methodological procedure

The procedure we developed to identify the sub-regions of M1 has several advantages. First, the identification of ROIs was both individual specific and consistent across groups. Another advantage is that placing these ROIs in the WM ensures more reliable tracking because the principal diffusion directions are more certain in WM than in the cortex. Most importantly, these ROIs allowed us to separately track each pathway from the specific region of M1. Finally, analyzing diffusion measures at the level of both the pLIC and the WM immediately subjacent the cortex provided us with additional information about the tract structure. Of course, our sub-division of M1 is a simplified model because the descending motor pathways actually originate in overlapping body-part representations, located not only in M1, but also in the premotor, supplementary motor and somatosensory (post-central) regions (Murray and Coulter 1981; Nudo and Masterton 1990; Dum and Strick 1991, 2005; Porter and Lemon 1995). Nonetheless, this approach could still be useful for other experimental or clinical studies that aim to identify specific components of the descending motor pathways, for example, to examine effector-specific outcomes of rehabilitation. In the future, our approach could be combined with a functional task to identify the location and extent of each body-part representation more precisely. Given the inherent limitations of DTI metrics, future studies could also use more advanced techniques, such as neurite orientation dispersion and density imaging (NODDI) or AxCaliber to separately measure myelin thickness (g-ratio) or the axonal diameter, respectively (Ellerbrock and Mohammadi 2018; Zhang et al. 2012; Assaf et al. 2008).

Conclusions

In this paper, we developed a novel approach to compare descending motor pathways in dancers and musicians. We found that dancers have higher diffusivity values and larger tract volume across most regions, with evidence for increased fiber bundle fanning at the level of the cortex, and larger axon diameter at the level of the internal capsule. Conversely, musicians showed increased FA in the hand and trunk/arm tracts, indicating that they have increased coherence and packing of the fibers that specifically connect the effectors they trained over time. Correlations with age of start of training and performance on dance and music tasks indicate that these structural changes are directly linked to specialized training of dancers and musicians. Taken together, our findings support the hypothesis that different types of training have different effects on brain structure.

Acknowledgements We would like to thank our participants for their time, Jennifer Bailey, Emily Coffey and Jamila Andoh for their assistance in the recruiting and testing process. This work was funded by a grant from the Natural Sciences and Engineering Council of Canada (NSERC) to Dr. Krista Hyde (238670).

Funding This work was funded by a grant from the Natural Sciences and Engineering Council of Canada (NSERC) to Dr. Krista Hyde (238670).

Compliance with ethical standards

Conflict of interest The authors declare that they have no conflicts of interest.

Ethical approval All procedures performed in studies involving human participants were in accordance with the ethical standards of the institutional and research committee and were approved by the Research Ethics Board at the Montreal Neurological Institute and Hospital.

Informed consent Written informed consent was obtained from all participants included in the study. Participants were compensated for their participation.

Supplementary Material

Sample-specific template

A sample-specific template with its parcellation of GM and WM regions was created from the raw images in order to define the center of gravity (COG) of the hand motor regions and standardize some operations across the sample. For instance, a sample-specific parcellation of GM and WM, implemented with the Freesurfer's Desikan-Killiany Atlas, was automatically calculated on the sample-specific template to localize the precentral motor cortices to guide the regions of interests (ROIs) localization. To make the template, all individual raw brain images were first projected to Freesurfer's operational space, named conformed space, applying the Freesurfer's tool `recon_all`. With this command, the individual labels of the GM and WM parcellated regions, necessary at different steps of the seed mask creation, were also produced. With a combination of Freesurfer's and FSL's tools, the structural brain images were transformed into the MNI152 standard space and averaged to constitute the sample-specific template in the MNI space.

More specifically, the brain structural images were transformed from the structural space (5a) to the MNI space (5b) with linear and nonlinear transformations, using FSL's FLIRT and FNIRT tools. They were then averaged, with FSL's `Fslmaths` tool, in the MNI space (5c) and transformed into the conformed space (5d) with `recon-all`, which also created the GM and WM parcellations of the template.

Seed mask creation

In order to separately track the primary motor pathways connecting the head, hand, trunk or leg representations, we defined, in each hemisphere, the four WM regions subjacent the motor cortex that topographically correspond to the head, hand, trunk/arm or leg/foot representations. To do this, we developed a procedure that permits to define the seed masks for tractography, using an approach that is at the same time sample-specific and reproducible across subjects. See the diagram in Fig. 6 for the procedure followed.

Creation of sample-specific hand centers of gravity (COGs)

The hand is the only body part whose topographical location within the motor cortex that can be identified using well-established gross anatomical landmarks (Yousry et al. 1997; Caulo et al. 2007). Therefore, the first step was to identify the hand motor region individually, create a sphere based on its center of gravity (COG) and then to locate the other body parts along M1 relative to its position. Hand motor regions for each individual were manually labeled in three dimensions for both hemispheres in Freesurfer's conformed space (7a). To do this, we overlaid the GM label of the precentral cortex provided by the Desikan-Killiany Atlas on each individual structural brain. To create the hand masks, we identified the hand regions defined by the hand landmarks, previously described as an omega or epsilon shaped portion of the cortex, with their variants (Yousry et al. 1997; Caulo et al. 2007). The user-drawn hand regions were then nonlinearly projected onto the MNI152 standard space with the FSL's tool `applywarp` (7b). The hand masks were then averaged (7c), with the FSL's tool `Fslmaths`, and projected

Fig. 5 Template creation. **a** Individual structural brain image. **b** Individual brain image in MNI space. **c** Averaged brain image in MNI space. **d** Averaged brain image in conformed space, i.e., template

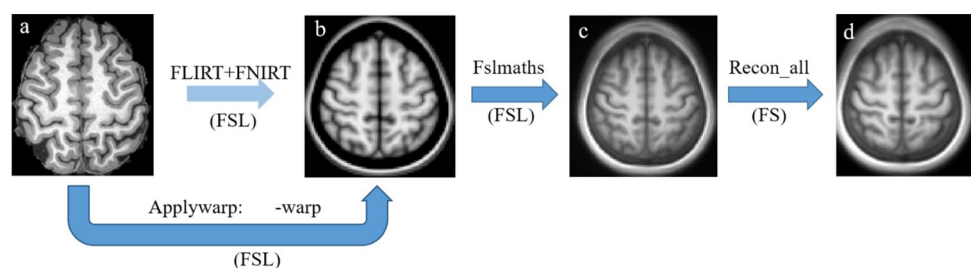


Fig. 6 Diagram of the steps followed to create the seed masks. The yellow windows indicate the user-defined steps; the light orange windows indicate the steps that were standardized across subjects



again onto the sample-specific template space (7d), using the Freesurfer's tool `mri_vol2vol`. Finally, the COGs of the average hand masks were calculated, in the template conformed space, using the FSL's tool `Fslstats`.

Creation of seed masks from COGs across subjects

Once the hand COGs were calculated, the appropriate radii were estimated to draw the hand spheres around them. These parcellations were critical as visual checks for the determination of the radii of the spheres, allowing us to ensure that the spheres included all the relevant portions of the precentral cortex parcellation (Desikan-Killiany Atlas).

The trunk, leg and hand spheres were created relative to the hand sphere positions by shifting the hand COGs along the precentral cortex (Table 4). In particular, the trunk sphere was entirely shifted along the x-direction medially, so that the sphere included a similar portion of the cortex with minimal overlapping. For the leg and head, the spheres were first shifted along the x-direction—medially and laterally, respectively—and then along the z-direction (both spheres) and the y-direction (head sphere only), in order to include all the cortex.

The radii were also adjusted to include all the relevant portion of the precentral motor cortex. In the end, the hand and trunk spheres had the same radii, whereas the leg and

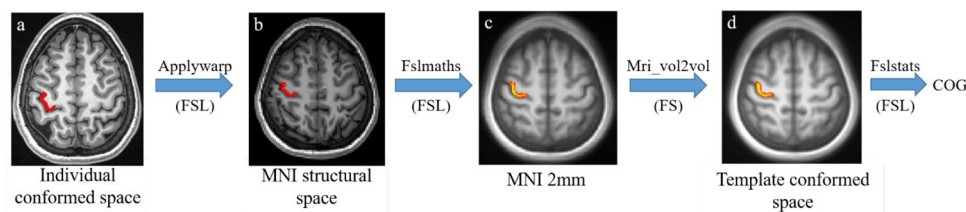


Fig. 7 Calculation of the hand center of gravity (COG) for the right hemisphere, from manually drawn hand ROIs. **a** Individual manually drawn hand ROI in the subject Freesurfer's conformed space. **b** Individual manually drawn hand ROI in the MNI structural space. **c** Aver-

age of all subjects manually drawn hand ROIs in MNI 2 mm space. **d** Average of manually drawn hand ROIs in template conformed space (thresholded at 30%)

Table 4 Coordinates of the centers of gravity (COGs) in the MNI space (mm) for the four motor regions

	Right			Left			Radius (mm)
	COG x (mm)	COG y (mm)	COG z (mm)	COG x (mm)	COG y (mm)	COG z (mm)	
Head	49	3	25	-46	3	25	24
Hand	37	-19	60	-35	-21	61	15
Trunk	14	-25	66	-13	-25	66	15
Leg	13	-25	54	-13	-25	54	21

the head regions, being more elongated, had bigger radii. Because there was some overlap between the hand and the trunk spheres, the trunk spheres were subtracted from the hand spheres; this was not necessary for the other spheres. While the hand, head and trunk spheres were masked with the precentral WM parcellation (see below), the leg spheres were masked with the paracentral WM parcellation; therefore there was no problematic overlapping with the trunk regions. It is worth noting that the paracentral WM underlies both the pre- and post-central cortices, and therefore, the leg tracts were not restricted to the descending primary motor fibers, but included also the ascending sensorimotor fibers.

Once obtained the bilateral COGs and spheres, we projected the spheres onto the structural subject space and masked them with the individual precentral WM masks. The choice of masking the spheres with the individual WM masks was done to take advantage of the more precise individual parcellations compared to the template parcellation.

In detail, the spheres were projected from the template conformed space (Fig. 7a) into the standard MNI152 space (Fig. 7b) applying the `mri_vol2vol` tool by Freesurfer. In this passage, the transformation matrix came from the previously calculated projection of the MNI space to the template conformed space, performed with `tkregister`, and was here inverted with the `-inv` option. A nonlinear warping procedure was then applied to project the spheres from the MNI space (Fig. 3b) to the individual structural space (Fig. 7c), using `applywarp` fed with linear and nonlinear warping, previously calculated with FLIRT and FNIRT. Then, by means of `Fslmaths` (`-mas` option), the spheres were masked with the WM individual parcellation in the structural space, previously transformed from the individual conformed space with FLIRT. Finally, the selected WM ROIs were projected onto the diffusion FA space with a linear transformation (FLIRT). The WM ROIs in FA space were now ready to be used as seed masks for tractography (Fig. 8).

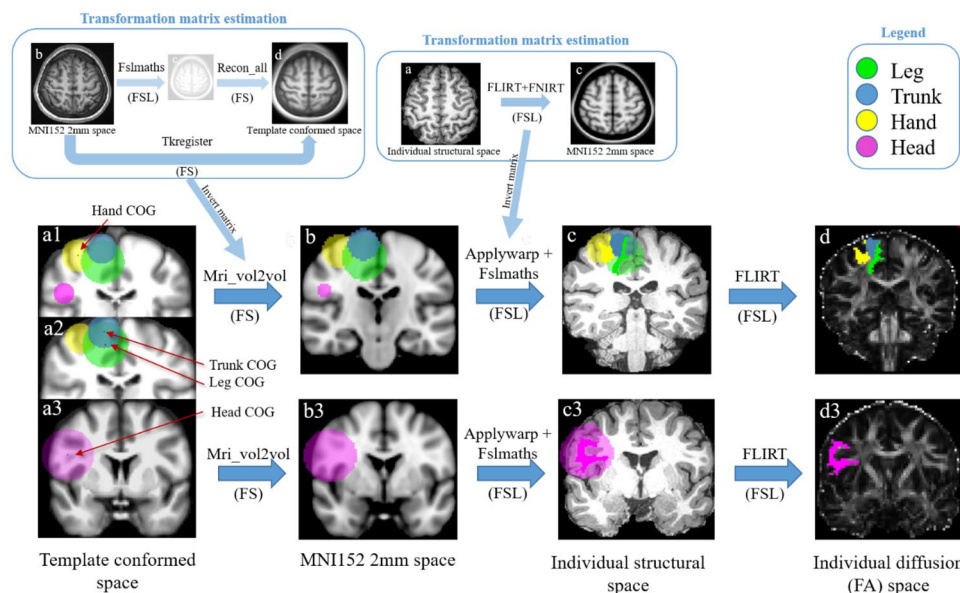


Fig. 8 Seed mask creation from spheres to final masks in the right hemisphere. **a** Spheres and COGs are shown in the template conformed space for the hand (yellow sphere, COG indicated by red arrow in a1), trunk (light blue sphere, COG in a2), leg (green sphere, COG in a2) and head (fuchsia sphere, COG in a3). **b** Spheres in MNI152 space. **c** Spheres in one subject individual structural space overlapping with the precentral/paracentral cortex; bottom row shows the head transformation not visible in the same slice as the other body-part regions. **d** Individual final seed masks in one subject FA

diffusion space. The light blue arrows between images indicate the transformations between images, the commands used, above the arrow, and the software, below the arrows (FSL and Freesurfer, FS). Above the main images transformations, the transformation matrix estimations are shown to indicate where the transformation matrices come from. For instance, to project the spheres from the template space to the MNI space, the inverted matrix created with the command `tkregister` from the MNI space to the template conformed space was applied (see Fig. 5b in [Supplementary Material](#)→d)

References

- Acer N, Bastepe-Gray S, Sagioglu A, Gumus KZ, Degirmencioglu L, Zararsiz G, Ozic MU (2018) Diffusion tensor and volumetric magnetic resonance imaging findings in the brains of professional musicians. *J Chem Neuroanat* 88:33–40. <https://doi.org/10.1016/j.jchemneu.2017.11.003>
- Andersson JLR, Jenkinson M, Smith S (2007) Non-linear registration aka Spatial normalisation, FMRIB Technical Report TR07JA2. Tech. rep, FMRIB Centre, Oxford, United Kingdom
- Andoh J, Matsushita R, Zatorre RJ (2015) Asymmetric interhemispheric transfer in the auditory network: evidence from TMS, resting-state fMRI, and diffusion imaging. *J Neurosci* 35:14602–14611. <https://doi.org/10.1523/JNEUROSCI.2333-15.2015>
- Assaf Y, Blumenfeld-Katzir T, Yovel Y, Basser PJ (2008) AxCaliber: a method for measuring axon diameter distribution from diffusion MRI. *Magn Reson Med* 59(6):1347–1354. [10.1002/mrm.21577](https://doi.org/10.1002/mrm.21577), <http://www.ncbi.nlm.nih.gov/pubmed/18506799>
- Bailey J, Penhune V (2010) Rhythm synchronization performance and auditory working memory in early- and late-trained musicians. *Exp Brain Res* 204(1):91–101. <https://doi.org/10.1007/s00221-010-2299-y>
- Bailey JA, Zatorre RJ, Penhune VB (2014) Early musical training is linked to gray matter structure in the ventral premotor cortex and auditory-motor rhythm synchronization performance. *J Cognit Neurosci* 26(4):755–767. https://doi.org/10.1162/jocn_a_00527
- Basser P, Mattiello J, LeBihan D (1994) MR diffusion tensor spectroscopy and imaging. *Biophys J* 66(1):259–267. [https://doi.org/10.1016/S0006-3495\(94\)80775-1](https://doi.org/10.1016/S0006-3495(94)80775-1)
- Behrens TE, Woolrich MW, Jenkinson M, Johansen-Berg H, Nunes RG, Clare S, Matthews PM, Brady JM, Smith SM (2003) Characterization and propagation of uncertainty in diffusion-weighted MR imaging. *Magn Reson Med* 50:1077–1088. <https://doi.org/10.1002/mrm.10609>
- Behrens TE, Berg HJ, Jbabdi S, Rushworth MF, Woolrich MW (2007) Probabilistic diffusion tractography with multiple fibre orientations: What can we gain? *NeuroImage* 34:144–155. <https://doi.org/10.1016/j.neuroimage.2006.09.018>
- Bengtsson SL, Nagy Z, Skare S, Forsman L, Forsberg H, Ullén F (2005) Extensive piano practicing has regionally specific effects on white matter development. *Nat Neurosci* 8(9):1148–1150. <https://doi.org/10.1038/nm1516>
- Bezzola L, Merillat S, Gaser C, Jancke L (2011) Training-induced neural plasticity in golf novices. *J Neurosci* 31(35):12444–12448. [10.1523/JNEUROSCI.1996-11.2011](https://doi.org/10.1523/JNEUROSCI.1996-11.2011), http://www.ncbi.nlm.nih.gov/entrez/query.fcgi?cmd=Retrieve&db=PubMed&dopt=Citation&list_uids=21880905
- Burzynska AZ, Finc K, Taylor BK, Knecht AM, Kramer AF (2017) The dancing brain: structural and functional signatures of expert dance training. *Front Hum Neurosci* 11:566. <https://doi.org/10.3389/fnhum.2017.00566>
- Caulo M, Briganti C, Mattei PA, Perfetti B, Ferretti A, Romani GL, Tartaro A, Colosimo C (2007) New morphologic variants of the hand motor cortex as seen with MR imaging in a large study population. *Am J Neuroradiol* 28:1480–1485. <https://doi.org/10.3174/ajnr.A0597>
- Chéreau R, Saraceno GE, Angibaud J, Cattaert D, Nägerl UV (2017) Superresolution imaging reveals activity-dependent plasticity of axon morphology linked to changes in action potential conduction velocity. *Proc Natl Acad Sci* 114(6):1401–1406. <https://doi.org/10.1073/pnas.1607541114>
- Choi US, Sung YW, Hong S, Chung JY, Ogawa S (2015) Structural and functional plasticity specific to musical training with wind instruments. *Front Hum Neurosci* 9:597. <https://doi.org/10.3389/fnhum.2015.00597>
- Coffey EBJ, Herholz SC, Scala S, Zatorre RJ (2011) The Montreal Music History Questionnaire: a tool for the assessment of music-related experience in music cognition research. In: *Neurosciences and music IV: learning and memory*, Edinburgh, UK
- Desikan RS, Ségonne F, Fischl B, Quinn BT, Dickerson BC, Blacker D, Buckner RL, Dale AM, Maguire RP, Hyman BT, Albert MS, Killiany RJ (2006) An automated labeling system for subdividing the human cerebral cortex on MRI scans into gyral based regions of interest. *NeuroImage* 31(3):968–980. <https://doi.org/10.1016/j.neuroimage.2006.01.021>
- Draganski B, Gaser C, Busch V, Schuierer G, Bogdahn U, May A (2004) Neuroplasticity: changes in grey matter induced by training. *Nature* 427(6972):311–312. [10.1038/427311a427311a1a](https://doi.org/10.1038/427311a427311a1a)[pii], http://www.ncbi.nlm.nih.gov/entrez/query.fcgi?cmd=Retrieve&db=PubMed&dopt=Citation&list_uids=14737157
- Dum RP, Strick PL (1991) The origin of corticospinal projections from the premotor areas in the frontal lobe. *J Neurosci* 11(3):667–89
- Dum RP, Strick PL (2005) Frontal lobe inputs to the digit representations of the motor areas on the lateral surface of the hemisphere. *J Neurosci* 25(6):1375–1386. <https://doi.org/10.1523/JNEUROSCI.3902-04.2005>
- Elbert T, Pantev C, Wienbruch C, Rockstroh B, Elbert T, Pantev C, Wienbruch C, Rockstroh B, Taub E (1995) Increased Cortical Representation of the Fingers of the Left Hand in String Players Edward Taub Published by: American Association for the Advancement of Science Stable URL: <https://www.jstor.org/stable/2888544> digitize, preserve and extend access to *Science* 270(5234):305–307
- Ellerbrock I, Mohammadi S (2018) Four in vivo g-ratio-weighted imaging methods: comparability and repeatability at the group level. *Human Brain Mapping* 39(1):24–41. <https://doi.org/10.1002/hbm.23858>, <http://www.ncbi.nlm.nih.gov/pubmed/29091341>
- Foster NE, Zatorre RJ (2010) Cortical structure predicts success in performing musical transformation judgments. *Neuroimage* 53(1):26–36. [10.1016/j.neuroimage.2010.06.042](https://doi.org/10.1016/j.neuroimage.2010.06.042), http://www.ncbi.nlm.nih.gov/entrez/query.fcgi?cmd=Retrieve&db=PubMed&dopt=Citation&list_uids=20600982
- Gaser C, Schlaug G (2003) Gray matter differences between musicians and nonmusicians. *Ann N Y Acad Sci* 999:514–517. http://www.ncbi.nlm.nih.gov/entrez/query.fcgi?cmd=Retrieve&db=PubMed&dopt=Citation&list_uids=14681175
- Giacosa C, Karpati F, Foster N, Penhune VB, Hyde K (2016) Dance and music training have different effects on white matter diffusivity in sensorimotor pathways. *NeuroImage* 135:273–286. <https://doi.org/10.1016/j.neuroimage.2016.04.048>
- Giorgio A, Watkins KE, Chadwick M, James S, Winmill L, Douaud G, De Stefano N, Matthews PM, Smith SM, Johansen-Berg H, James AC (2010) Longitudinal changes in grey and white matter during adolescence. *NeuroImage*. 49:94–103. <https://doi.org/10.1016/j.neuroimage.2009.08.003>
- Halwani GF, Loui P, Rüber T, Schlaug G (2011) Effects of practice and experience on the arcuate fasciculus: comparing singers, instrumentalists, and non-musicians. *Front Psychol* 2:156. <https://doi.org/10.3389/fpsyg.2011.00156>, http://www.ncbi.nlm.nih.gov/entrez/query.fcgi?cmd=Retrieve&db=PubMed&dopt=Citation&list_uids=21779271
- Hammond G (2002) Correlates of human handedness in primary motor cortex: a review and hypothesis. *Neurosci Biobehav Rev* 26(3):285–292. [https://doi.org/10.1016/S0149-7634\(02\)00003-9](https://doi.org/10.1016/S0149-7634(02)00003-9)
- Han Y, Yang H, Lv YT, Zhu CZ, He Y, Tang HH, Gong QY, Luo YJ, Zang YF, Dong Q (2009) Gray matter density and white matter integrity in pianists' brain: a combined structural and

- diffusion tensor MRI study. *Neurosci Lett* 459(1):3–6. <https://doi.org/10.1016/j.neulet.2008.07.056>
- Hänggi J, Koeneke S, Bezzola L, Jancke L (2010) Structural neuroplasticity in the sensorimotor network of professional female ballet dancers. *Hum Brain Mapp* 31(8):1196–1206. <https://doi.org/10.1002/hbm.20928>. http://www.ncbi.nlm.nih.gov/entrez/query.fcgi?cmd=Retrieve&db=PubMed&dopt=Citation&list_uids=20024944
- Harrington B, Alan Fine G (2000) Opening the “black box”: Small groups and twenty-first-century sociology. *Social Psychology Quarterly* 63(4):312–323. <https://www.scholars.northwestern.edu/en/publications/opening-the-black-box-small-groups-and-twenty-first-century-socio>
- Horenstein C, Lowe MJ, Koenig KA, Phillips MD (2009) Comparison of unilateral and bilateral complex finger tapping-related activation in premotor and primary motor cortex. *Hum Brain Mapp* 30(4):1397–1412. [10.1002/hbm.20610](https://doi.org/10.1002/hbm.20610), <http://www.ncbi.nlm.nih.gov/pubmed/18537112>
- Huang R, Lu M, Song Z, Wang J (2013) Long-term intensive training induced brain structural changes in world class gymnasts. *Brain Struct Funct* 220(2):625–644. <https://doi.org/10.1007/s00429-013-0677-5>
- Imfeld A, Oechslin MS, Meyer M, Loenneker T, Jancke L (2009) White matter plasticity in the corticospinal tract of musicians: a diffusion tensor imaging study. *Neuroimage* 46(3):600–607. <https://doi.org/10.1016/j.neuroimage.2009.02.025>, http://www.ncbi.nlm.nih.gov/entrez/query.fcgi?cmd=Retrieve&db=PubMed&dopt=Citation&list_uids=19264144
- Jäncke L, Koeneke S, Hoppe A, Rominger C, Hänggi J (2009) The architecture of the Golfer’s brain. *PLoS One* 4(3):e4785. <https://doi.org/10.1371/journal.pone.0004785>
- Jenkinson M, Smith S (2001) A global optimisation method for robust affine registration of brain images. *Med Image Anal* 5(2):143–56
- Jenkinson M, Bannister P, Brady M, Smith S (2002) Improved optimization for the robust and accurate linear registration and motion correction of brain images. *NeuroImage* 17(2):825–41
- Karni A, Meyer G, Jezzard P, Adams MM, Turner R, Ungerleider LG (1995) Functional MRI evidence for adult motor cortex plasticity during motor skill learning. *Nature* 377(6545):155–158. <https://doi.org/10.1038/377155a0>
- Karpati F, Giacosa C, Foster N, Penhune VB, Hyde K (2016) Sensorimotor integration is enhanced in dancers and musicians. *Exp Brain Res* 234(3):893–903. <https://doi.org/10.1007/s00221-015-4524-1>
- Karpati F, Giacosa C, Foster N, Penhune VB, Hyde K (2017) Dance and music share gray matter structural correlates. *Brain Res* 1657:62–73. <https://doi.org/10.1016/j.brainres.2016.11.029>
- Karpati F, Giacosa C, Foster N, Penhune VB, Hyde K (2018) Structural covariance analysis reveals differences between dancers and untrained controls. *Front Hum Neurosci* 12:373. <https://doi.org/10.3389/fnhum.2018.00373>
- Kleim JA, Barbay S, Nudo RJ (1998) Functional reorganization of the rat motor cortex following motor skill learning. *J Neurophysiol* 80(6):3321–3325. <https://doi.org/10.1152/jn.1998.80.6.3321>
- Kleim JA, Barbay S, Cooper NR, Hogg TM, Reidel CN, Remple MS, Nudo RJ (2002) Motor learning-dependent synaptogenesis is localized to functionally reorganized motor cortex. *Neurobiol Learn Mem* 77(1):63–77. <https://doi.org/10.1006/nlme.2000.4004>
- Madhyastha T, Méritat S, Hirsiger S, Bezzola L, Liem F, Grabowski T, Jäncke L (2014) Longitudinal reliability of tract-based spatial statistics in diffusion tensor imaging. *Hum Brain Mapp* 35:4544–4555. <https://doi.org/10.1002/hbm.22493>
- Meier J, Topka MS, Hänggi J (2016) Differences in cortical representation and structural connectivity of hands and feet between professional handball players and ballet dancers. *Neural Plast* 2016:6817397. <https://doi.org/10.1155/2016/6817397>
- Morgen K, Kadom N, Sawaki L, Tessitore A, Ohayon J, Frank J, McFarland H, Martin R, Cohen LG (2004) Kinematic specificity of cortical reorganization associated with motor training. *NeuroImage* 21:1182–1187. <https://doi.org/10.1016/j.neuroimage.2003.11.006>
- Mori S, Crain B (2005) MRI atlas of human white matter, 6th edn. Elsevier, Amsterdam
- Murray EA, Coulter JD (1981) Organization of corticospinal neurons in the monkey. *J Comp Neurol* 195(2):339–65. <https://doi.org/10.1002/cne.901950212>
- Noble JW, Eng JJ, Boyd LA (2014) Bilateral motor tasks involve more brain regions and higher neural activation than unilateral tasks: an fMRI study. *Exp Brain Res* 232(9):2785–2795. <https://doi.org/10.1007/s00221-014-3963-4>
- Nudo RJ, Masterton RB (1990) Descending pathways to the spinal cord, III: sites of origin of the corticospinal tract. *J Comp Neurol* 296(4):559–583. <https://doi.org/10.1002/cne.902960405>
- Nudo RJ, Milliken GW, Jenkins WM, Merzenich MM (1996) Use-dependent alterations of movement representations in primary motor cortex of adult squirrel monkeys. *J Neurosci* 16(2):785–807. <http://www.ncbi.nlm.nih.gov/pubmed/8551360>
- O’Donnell LJ, Pasternak O (2015) Does diffusion MRI tell us anything about the white matter? An overview of methods and pitfalls. *Schizophrenia Res* 161(1):133–141. <https://doi.org/10.1016/j.SCHRES.2014.09.007>
- Oechslin MS, Gschwind M, James CE (2017) Tracking training-related plasticity by combining fMRI and DTI: the right hemisphere ventral stream mediates musical syntax processing. *Cereb Cortex* 28(4):1209–1218. <https://doi.org/10.1093/cercor/bhx033>
- Pantev C, Engelien A, Candia V, Elbert T (2001) Representational cortex in musicians. Plastic alterations in response to musical practice. *Ann N Y Acad Sci* 930:300–14. <https://doi.org/10.1111/j.1749-6632.2001.tb05740.x>
- Penhune VB (2019) Musical expertise and brain structure: the causes and consequences of training. In: Thaut MH, Hodges DA (eds) *The Oxford handbook of music and the brain*, pp 1–22. <https://doi.org/10.1093/oxfordhb/9780198804123.013.17>
- Porter R, Lemon R (1995) Anatomical substrates for movement performance: cerebral cortex and the corticospinal tract. In: *Corticospinal function and voluntary movement*. Monographs of the physiological society no 45. Clarendon Press/Oxford University Press, Oxford, New York, pp 36–89. <https://doi.org/10.1093/acprof:oso/9780198523758.003.0002>
- Rüber T, Lindenberg R, Schlaug G (2013) Differential adaptation of descending motor tracts in musicians. *Cereb Cortex* 25(6):1490–1498. <https://doi.org/10.1093/cercor/bht331>
- Rüber T, Lindenberg R, Schlaug G (2015) Differential adaptation of descending motor tracts in musicians. *Cereb Cortex* 25(6):1490–1498. <https://doi.org/10.1093/cercor/bht331>
- Salat DH, Greve DN, Pacheco JL, Quinn BT, Helmer KG, Buckner RL, Fischl B (2009) Regional white matter volume differences in nondemented aging and Alzheimer’s disease. *NeuroImage* 44:1247–1258. <https://doi.org/10.1016/j.neuroimage.2008.10.030>
- Sampaio-Baptista C, Johansen-Berg H (2017) White matter plasticity in the adult brain. *Neuron* 96(6):1239–1251. <https://doi.org/10.1016/j.neuron.2017.11.026>
- Sampaio-Baptista C, Khrapitchev AA, Foxley S, Schlagheck T, Scholz J, Jbabdi S, DeLuca GC, Miller KL, Taylor A, Thomas N, Kleim J, Sibson NR, Bannerman D, Johansen-Berg H (2013) Motor skill learning induces changes in white matter microstructure and myelination. *J Neurosci* 33(50):19499–19503. <https://doi.org/10.1523/JNEUROSCI.3048-13.2013>
- Schlaffke L, Lissek S, Lenz M, Brüne M, Juckel G, Hinrichs T, Platen P, Tegenthoff M, Schmidt-Wilcke T (2014) Sports and brain

- morphology—a voxel-based morphometry study with endurance athletes and martial artists. *Neuroscience* 259:35–42. <https://doi.org/10.1016/j.neuroscience.2013.11.046>
- Schlaug G, Jäncke L, Huang Y, Staiger JF, Steinmetz H (1995) Increased corpus callosum size in musicians. *Neuropsychologia* 33(8):1047–55
- Schmithorst VJ, Wilke M (2002) Differences in white matter architecture between musicians and non-musicians: a diffusion tensor imaging study. *Neurosci Lett* 321(1–2):57–60, DOI S030439400200054X[pii], http://www.ncbi.nlm.nih.gov/entrez/query.fcgi?cmd=Retrieve&db=PubMed&dopt=Citation&list_uids=11872256
- Scholz J, Klein MC, Behrens TE, Johansen-berg H (2009) Training induces changes in white matter architecture. *Nat Neurosci* 12(11):1370–1371. <https://doi.org/10.1038/nn.2412>
- Sehm B, Steele CJ, Villringer A, Ragert P (2016) Mirror motor activity during right-hand contractions and its relation to white matter in the posterior midbody of the corpus callosum. *Cereb Cortex* 26(11):4347–4355. <https://doi.org/10.1093/cercor/bhv217>
- Smith SM (2002) Fast robust automated brain extraction. *Hum Brain Mapp* 17(3):143–155. <https://doi.org/10.1002/hbm.10062>
- Steele CJ, Bailey JA, Zatorre RJ, Penhune VB (2013) Early Musical Training and White-Matter Plasticity in the Corpus Callosum: Evidence for a Sensitive Period. *J Neurosci* 33(3):1282–1290. <https://doi.org/10.1523/JNEUROSCI.3578-12.2013>, <http://www.jneurosci.org/cgi/doi/10.1523/JNEUROSCI.3578-12.2013>
- Taubert M, Draganski B, Anwander A, Müller K, Horstmann A, Villringer A, Ragert P (2010) Dynamic Properties of Human Brain Structure: Learning-Related Changes in Cortical Areas and Associated Fiber Connections. *J Neurosci* 30(35):11670–11677. <https://doi.org/10.1523/JNEUROSCI.2567-10.2010>, <http://www.jneurosci.org/cgi/doi/10.1523/JNEUROSCI.2567-10.2010>
- Taubert M, Mehnert J, Pleger B, Villringer A (2016) Rapid and specific gray matter changes in M1 induced by balance training. *NeuroImage* 133:399–407. <https://doi.org/10.1016/j.neuroimage.2016.03.017>
- Tyč F, Boyadjian A, Devanne H (2005) Motor cortex plasticity induced by extensive training revealed by transcranial magnetic stimulation in human. *Euro J Neurosci* 21(1):259–266. <https://doi.org/10.1111/j.1460-9568.2004.03835.x>
- Vaalto S, Julkunen P, Säisänen L, Könönen M, Määttä S, Karhu J (2013) Long-term plasticity may be manifested as reduction or expansion of cortical representations of actively used muscles in motor skill specialists. *NeuroReport* 24(11):596–600. <https://doi.org/10.1097/WNR.0b013e3283628636>
- Verstynen T, Diedrichsen J, Albert N, Aparicio P, Ivry R (2005) Ipsilateral motor cortex activity during unimanual hand movements relates to task complexity. *J Neurophysiol* 93:1209–1222. <https://doi.org/10.1152/jn.00720.2004>
- Wan CY, Schlaug G (2010) Music making as a tool for promoting brain plasticity across the life span. *Neuroscientist* 16(5):566–577. <https://doi.org/10.1177/1073858410377805>
- Wang B, Fan Y, Lu M, Li S, Song Z, Peng X, Zhang R, Lin Q, He Y, Wang J, Huang R (2013) Brain anatomical networks in world class gymnasts: A DTI tractography study. *NeuroImage* 65:476–487. <https://doi.org/10.1016/j.neuroimage.2012.10.007>
- Yousry TA, Schmid UD, Alkadhi H, Schmidt D, Peraud A, Büttner A, Winkler P (1997) Localization of the motor hand area to a knob on the precentral gyrus a new landmark. *Brain* 120:141–157
- Zatorre RJ, Fields RD, Johansen-Berg H (2012) Plasticity in gray and white: neuroimaging changes in brain structure during learning. *Nature Neurosci* 15(4):528–536. <https://doi.org/10.1038/nn.3045>
- Zhang H, Schneider T, Wheeler-Kingshott CA, Alexander DC (2012) NODDI: practical in vivo neurite orientation dispersion and density imaging of the human brain. *NeuroImage* 61(4):1000–1016. <https://doi.org/10.1016/j.neuroimage.2012.03.072>

Publisher's Note Springer Nature remains neutral with regard to jurisdictional claims in published maps and institutional affiliations.